



UNIVERSITY OF LEEDS

This is a repository copy of *Inorganic mineral precipitation from potable water on heat transfer surfaces*.

White Rose Research Online URL for this paper:
<http://eprints.whiterose.ac.uk/158884/>

Version: Accepted Version

Article:

Al-Gailani, A orcid.org/0000-0001-9290-0636, Charpentier, TVJ, Sanni, O orcid.org/0000-0002-3895-7532 et al. (3 more authors) (2020) Inorganic mineral precipitation from potable water on heat transfer surfaces. *Journal of Crystal Growth*, 537. 125621. ISSN 0022-0248

<https://doi.org/10.1016/j.jcrysgro.2020.125621>

© 2020, Elsevier. All rights reserved. This manuscript version is made available under the CC-BY-NC-ND 4.0 license <http://creativecommons.org/licenses/by-nc-nd/4.0/>.

Reuse

This article is distributed under the terms of the Creative Commons Attribution-NonCommercial-NoDerivs (CC BY-NC-ND) licence. This licence only allows you to download this work and share it with others as long as you credit the authors, but you can't change the article in any way or use it commercially. More information and the full terms of the licence here: <https://creativecommons.org/licenses/>

Takedown

If you consider content in White Rose Research Online to be in breach of UK law, please notify us by emailing eprints@whiterose.ac.uk including the URL of the record and the reason for the withdrawal request.



eprints@whiterose.ac.uk
<https://eprints.whiterose.ac.uk/>

Inorganic Mineral Precipitation from Potable Water on Heat Transfer Surfaces

Amthal Al-Gailani^{1*}, Thibaut V. J. Charpentier², Olujide Sanni¹, Richard Crisp³, Jantinus H. Bruins⁴ and Anne Neville¹

¹ *School of Mechanical Engineering, University of Leeds, Leeds, LS2 9JT, England*

² *School of Chemical and Process Engineering (SCAPE), University of Leeds, Leeds, LS2 9JT, England*

³ *Fernox Limited, Woking, Surrey, GU21 5RW, England*

⁴ *WLN, Glimmen, 9756 AD, Netherlands*

Abstract

In this study, an experimental approach mimicking processes encountered in electric kettles has been designed to investigate the influence of heating and cooling rate, and water composition on the kinetics of inorganic salt precipitation taking place when water is heated from ambient temperature up to its boiling point. The kinetics of salt precipitation in the bulk solution have been monitored through turbidity measurements as well as tracking ion concentration throughout the heating/ cooling process and the experimental findings highlight the critical role of the cooling step on the overall amount of salts that precipitate. The presence of magnesium ions in the water was found to influence the precipitation of calcium carbonate which was found to be the dominant salt crystallising out of solution; calcium sulphate was not observed.

Keywords: A1.Heat transfer; A2.Bulk crystallization; B1.Mineral precipitation; B1.Calcium carbonate; B1.Magnesium deposits.

1. Introduction

The precipitation of inorganic salts on surfaces is undoubtedly a serious heat transfer problem in water heating systems. Potable water used in domestic or industrial applications generally contains a variety of ions prone to precipitate over a range of concentrations depending on water quality and its geographic location. The formation of sparingly soluble inorganic deposits either in bulk solution or on heat transfer surfaces is a persistent and costly issue. It represents one of the major heat transfer and flow assurance problems in the oil sector, and water handling industry in general [1-6]. In households, scale formation has long been a concern in domestic appliances such as electric boilers, steam irons, washing machines, dishwashers, coffee makers and potable water distribution systems in general [7].

Scale build-up on the metallic surfaces of such appliances diminishes the heat transfer and increases the power needed to fulfil the desired performance. The deposition of inorganic salts can also result in reduced flow area which can lead to the failure of the domestic devices subjected to fouling. Moreover, the precipitation of salts in the bulk solution also affects the quality of the produced water such as taste and colour [8]. For instance, the suspended solids in the boiled water produced from coffee machines, kettles or instant water boilers may affect the taste of coffee, tea, etc. While the composition and quality of potable water vary based on geographic location [9], the heating of potable water is generally associated with the formation of various deposits with the most common being calcium carbonate (CaCO_3), calcium sulphate (CaSO_4), magnesium hydroxide ($\text{Mg}(\text{OH})_2$), and magnesium carbonate (MgCO_3) [10-12] (see Equations 1-3) with the resulting fouling layer made up of a mix of the aforementioned inorganic salts. When the water temperature rises from room temperature up to its boiling point, the solubility of inverse solubility salts decreases. This drop in solubility along with an increase in salinity due to water loss through evaporation during the heating process contributes to an increase in the thermodynamic driving force for the crystallisation reactions prompting the precipitation of salts out of solution [13]. Fig. 1 describes the process of salt precipitation as a function of time and temperature while Fig. 2 shows how the solubility product of CaCO_3 as calcite, MgCO_3 and CaSO_4 changes with temperature, respectively as derived from experimental studies [14, 15].

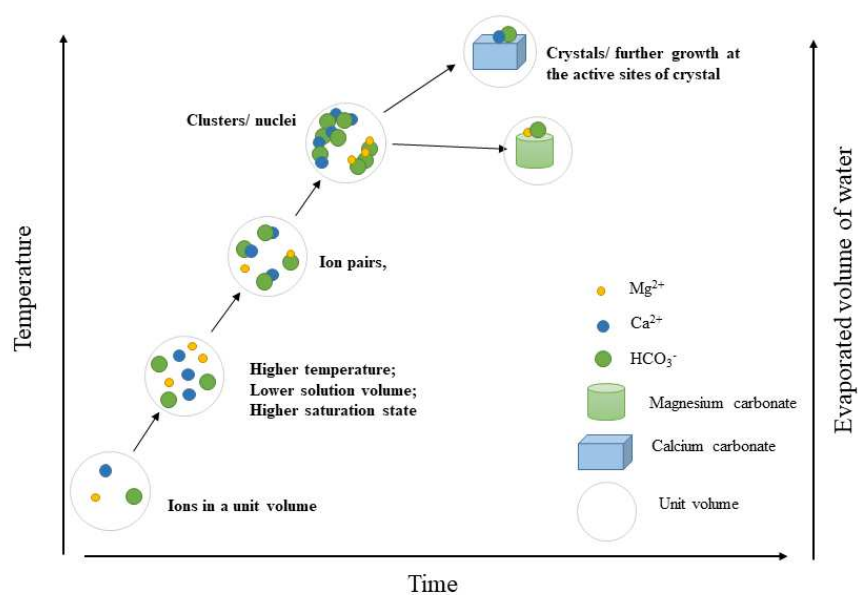
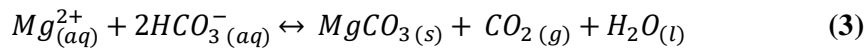
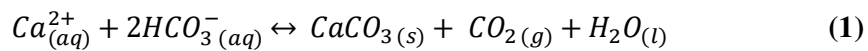


Fig. 1. Schematic drawing of composite precipitates formation from potable water.

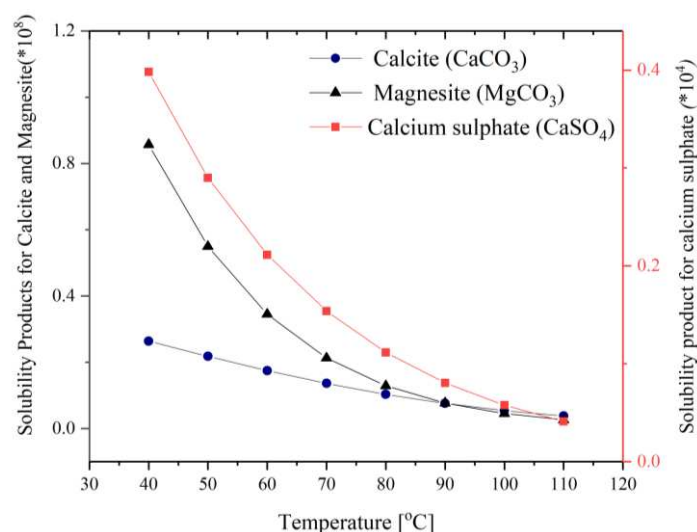


Fig. 2. Solubility of calcium carbonate forms and magnesium carbonate as a function of temperature.

The formation of inorganic scale in bulk solution has received a lot of attention in the literature over the last decades. However, most studies have focused on a narrow range of experimental conditions, generally using artificially hardened solutions to investigate the precipitation of one salt, under constant volume and temperature [16-19]. In the work reported herein, simultaneous precipitation of calcium carbonate, calcium sulphate and magnesium carbonate has been investigated by subjecting potable water to heating and cooling processes from room temperature up to its boiling point. The effect of heating rate on the crystallisation process has been assessed by monitoring the concentration of Ca^{2+} , SO_4^{2-} , and Mg^{2+} as a function of temperature and time.

2. Experimental methods

2.1. Test solution

The main solution used (solution A) in the experiments is a commercially available bottled water. It has been chosen rather than tap water, for its hardness of 307 ppm of CaCO_3 and pH of 7.2. Table 1 shows the composition of the solutions. The composition of solution A has been taken from the bottled label. However, the same batch has been analysed using the inductively coupled plasma atomic emission spectroscopy (ICP-OES). The analysis showed variation in some elements concentration such as calcium 94 mg/L, magnesium 30.8 mg/L and sulphate 10.4 mg/L.

Four other brines have been prepared to investigate the effect of water composition on the precipitation process. The concentrations of SO_4^{2-} and Ca^{2+} in solution B and Mg^{2+} in solution E have been chosen based on the drinking water quality report of the World Health Organization (WHO) [9]. All these four solutions were filtered using 20-25 μm filter paper to exclude the effect of impurities, and then a sample from each solution is taken to measure the initial value of pH and ion content.

Solution B is prepared by mixing 1.09 g/L of CaCl₂.6H₂O (Purity: 97 to 100%) (Honeywell Fluka) and 0.59 g/L of Na₂SO₄ (Purity: min. 99%) (VWR Chemicals) into deionized water. Solution C is made by mixing MgCl₂.6H₂O (Purity: 100%) (VWR Chemicals) and NaHCO₃ (Purity: 99.5%) (ACROS Organics) into deionized water. Finally, the solutions D and E are prepared by adding MgCl₂.6H₂O to solution A to obtain the magnesium content to 88 and 150 mg/L, respectively. The Saturation Ratio (*S*) of CaCO₃ and CaSO₄ has been calculated for each solution based on the initial concentrations of scale species at a temperature of 25 °C.

Table 1. Solution compositions.

| Ions (mg/L) | Solution A | Solution B | Solution C | Solution D | Solution E |
|---|-------------------|-------------------|-------------------|-------------------|-------------------|
| Ca ²⁺ | 80 | 200 | - | 80 | 80 |
| Mg ²⁺ | 26 | - | 26 | 88 | 150 |
| Na ⁺ | 6.5 | 183 | 130 | 6.5 | 6.5 |
| K ⁺ | 1 | - | - | 1 | 1 |
| Si ⁴⁺ | 15 | - | - | 15 | 15 |
| HCO ³⁻ | 360 | - | 360 | 360 | 360 |
| SO ₄ ²⁻ | 14 | 400 | - | 14 | 14 |
| Cl ⁻ | 10 | 350 | 84 | 177 | 361 |
| NO ³⁻ | 3.8 | - | - | 3.8 | 3.8 |
| Dry residue at 180°C | 345 | 780 | 413 | 502 | 546 |
| Initial saturation ratio of CaCO ₃ | 0.89 | - | - | 0.89 | 0.89 |
| Initial saturation ratio of CaSO ₄ | 0.007 | 0.52 | - | 0.007 | 0.007 |

2.2. Experimental setup and procedure

Experiments have been carried out in two different setups; namely, a lab-scale closed system and a commercially available electric kettle. The first setup consists of a 250 ml borosilicate vessel placed on a hot plate to provide the required heating. This simple setup is mimicking the heating process in some appliances such as kettles and uncomplicated coffee makers with a lower heating rate. To enhance the heating rate and to get to the boiling temperature in a shorter period, a silicone beaker heater with a power density of 0.008 W/mm² (BriskHeat, USA) has been used. The second apparatus is a kitchen electric kettle that has a capacity of 1700 ml and power of 3000 W. The heat is providing through a flat heating element in the bottom of the kettle.

The experimental procedure includes heating one of the solutions to its boiling temperature under atmospheric pressure. Once the heat source is switched on, solution sampling is regularly undertaken. By using a micropipette, 1 ml of the solution sample is mixed with 9 ml of a quenching solution made of 1 g of polyvinyl sulfonate (PVS) scale inhibitor and 5.71 g of KCl in 1000 ml of distilled water, then the pH was adjusted to a value between 8 – 8.5. The quenching was added for the purpose of preventing further crystallization in the solution. This 10 ml sample is used to assess the bulk concentration of cations (i.e., calcium, magnesium) by atomic absorption spectrophotometer (AAS) (Agilent Technologies, USA).

Other portions of the sample are also used to determine the solution pH and turbidity. The measurements of pH and turbidity of the solution are done using a HI 8014 Hanna pH-meter and DR-890 Colorimeter (CAMLAB, UK), respectively. The content of sulphate SO_4^{2-} in solution has been analysed using a spectrophotometer (DR3900, HACH, Lange, UK with sulphate cuvette test).

The different heating rates (Table 2) were achieved using the original beaker for the slow heating, the wrapped beaker for the medium heating, and finally the electric kettle to get the rapid heating. The heating rates were determined by the linear progression of the initial rising period of temperature (approximately between room temperature and 90 °C). Once attaining the boiling temperature, the heat source is switched off and the cooling rate investigations start. During the cooling stage, a solution sample is similarly taken at specific time steps. Table 3 shows the experimental configurations for the cooling rate experiments and temperature reduction rates. In the forced cooling experiment, the solution has been cooled in one litre jacketed vessel. Fresh tap water at room temperature is used as a coolant with no flow velocity. All tests of determining the effects of the heating and cooling rate are performed using solution A.

Table 2. Experimental setup for each heating rate

| Experimental configuration | Heating regime | Time to reach 100 °C | Heating rate (°C / min) |
|-----------------------------|----------------|----------------------|-------------------------|
| Uncovered beaker | Slow | 39 min | 3.19 |
| Heating band-wrapped beaker | Medium | 16 min | 6.35 |
| Electrical kettle | Rapid | 2.34 min | 30.6 |

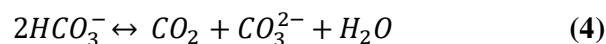
Table 3. Experimental setup for each cooling rate

| Experimental configuration | Heating regime | Cooling rate (°C/ min) |
|----------------------------|----------------|------------------------|
| Natural cooling | Slow | -0.9 |
| Forced cooling | Rapid | -7.39 |

3. Results and Discussion

3.1. Effect of heating rate

The temperature measurements in Fig. 3a show the time required to achieve water boiling temperature (100 °C) under atmospheric pressure. The solution pH is simultaneously measured. At all heating rates, the pH increases as time and temperature increase. It gives an indication of bicarbonate conversion to carbonate as well as the release of carbon dioxide as the temperature increases. The release of carbon dioxide from the evaporating solution influences the equilibrium of HCO_3^- and CO_3^{2-} ions by shifting the pH to higher values (Eq. 4). Hence, the formation of alkaline scales such as CaCO_3 , MgCO_3 and Mg(OH)_2 is more likely to occur [20]. Moreover, the temperature increases the dissociation constant of bicarbonate at constant water salinity [21]. The salinity can be determined by chloride ion concentration. It may also enhance the bicarbonate dissociation constant, thus the formation of carbonate species [22]. The chloride (Cl^-) ion content and the salinity increase with temperature and volume of evaporated water.



In the same period of heating, the calcium content in the solution has been reported in Fig. 3b. The findings show that the higher the heating rate the lower the amount of calcium consumed in the crystallisation reaction. The analysis of calcium ions concentration has been stopped when the bulk temperature reaches 100 °C. The solution contains 8.7, 52.4, and 66.1 mg/L of calcium in the slow, medium and rapid heating, respectively.

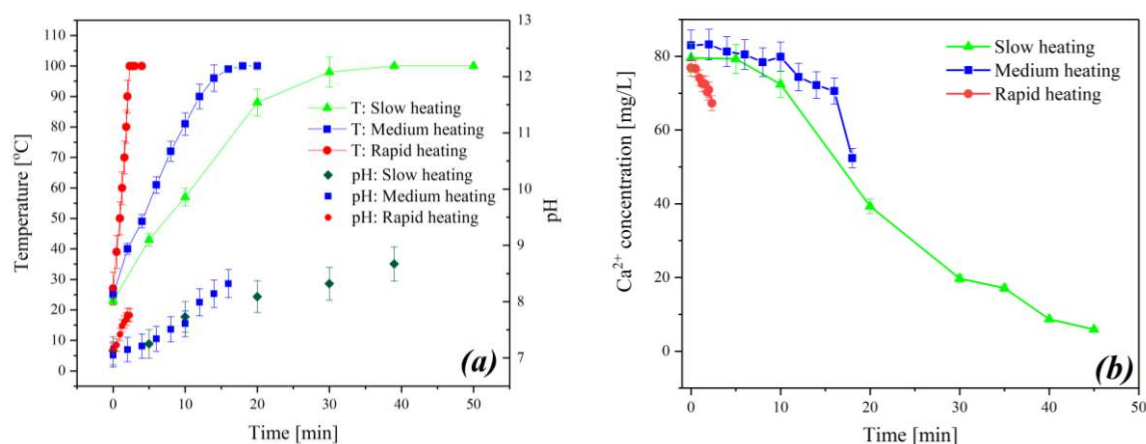


Fig. 3. (a) Profile of bulk temperature and pH, (b) profile of calcium concentration.

Fig. 4a displays the change of calcium concentration as a function of temperature in the heating process for different heating rates. Solution A was used as a test solution in the investigation of the effect of the heating rate. The highest concentration of Ca^{2+} at the boiling point is achieved by the rapid heating, while the lowest one is achieved by the slow heating. This implies more precipitation is formed when the solution is slowly heated. The solution turbidity has been determined with temperature increase as

shown in Fig.4b. The solution becomes more turbid at the boiling point when water is slowly heated. This confirms that the calcium undergoes a crystallisation reaction with carbonate. The slow heating of tap water from room temperature to boiling temperature allows the solid deposits to form. In other words, the longer heating time leads to a higher amount of inorganic scale.

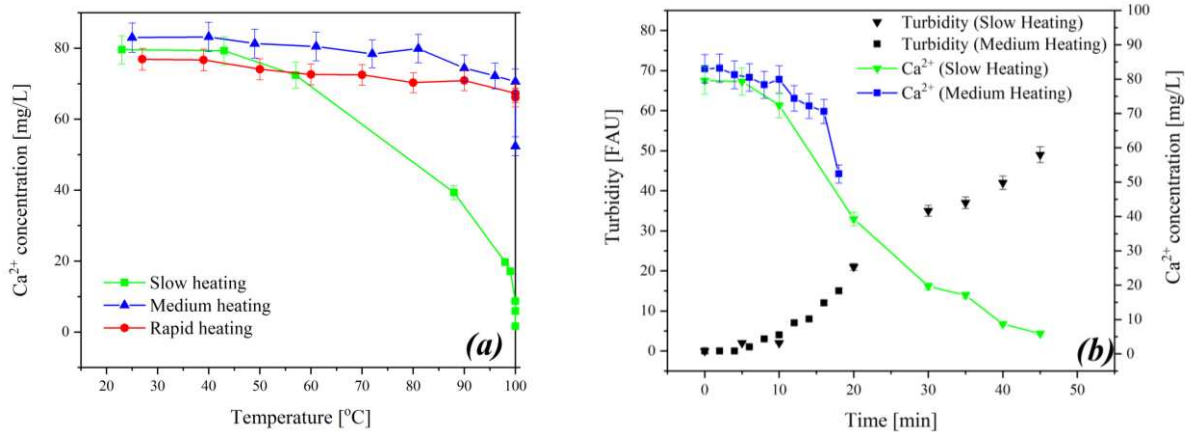


Fig. 4. (a) Change of calcium concentration with temperature, (b) change of solution turbidity with time.

The effect of heating rate on the rate of calcium ion consumption in the solution is summarized in Fig. 5. The rate of temperature change (is obtained by the linear fitting of the rising rate period in the (temperature-time) curve in Fig. 3a. Higher rate of temperature change leads to a faster reaction rate of calcium precipitation. However, in spite of the fact that the reaction rate is slower at the lower heating rate, the longer time is required to achieve the boiling point leading to a greater amount of precipitated salt. The temperature has an influence on the crystallisation reaction constant and rate of carbonate formation from bicarbonate, hence the overall reaction rate [23].

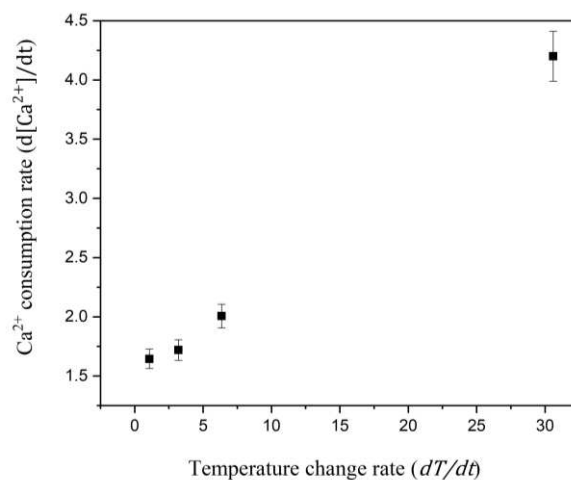


Fig. 5. Change of calcium reaction rate with heating rate.

3.2. Effect of cooling rate

The formation of inorganic deposits is not only expected in the heating period but also after cutting the heat source and leaving the solution to cool. The drop of temperature from 100 °C to about 45 °C due to heat loss to the surroundings is the second phase for the scale formation. The cooling rate affects the consumption rate of calcium and final content at 45 °C, as shown in Fig. 6a. Longer residence time at the temperature range where the crystallisation reaction is favourable results in a higher amount of precipitate. The mechanism of bulk precipitation during the cooling stage is different from that during the heating stage as it is affected by the solution temperature and the pre-existing scale crystals. The particles that formed in the heating stage can act as nucleation sites and promote heterogeneous nucleation [24].

The results in Fig. 6b illustrate how the Ca^{2+} content at slow cooling is lower than that at quick cooling for the same solution temperature. The solution pH for both cooling rates rises as the temperature decreases with little dependence on the cooling rate. Fig. 7a and Fig. 7b distinguish between the decay rates of calcium during the rapid heating and natural cooling for the commercially available electric kettle. The data has been linearly fitted to determine the rate of calcium consumption as a function of temperature in the heating and cooling cycles, respectively. It can be seen that the calcium ions are largely consumed in the cooling stage rather than that in the heating stage. In other words, the scale that forms when water is cooling is greater than heating as the time in the latter is much shorter.

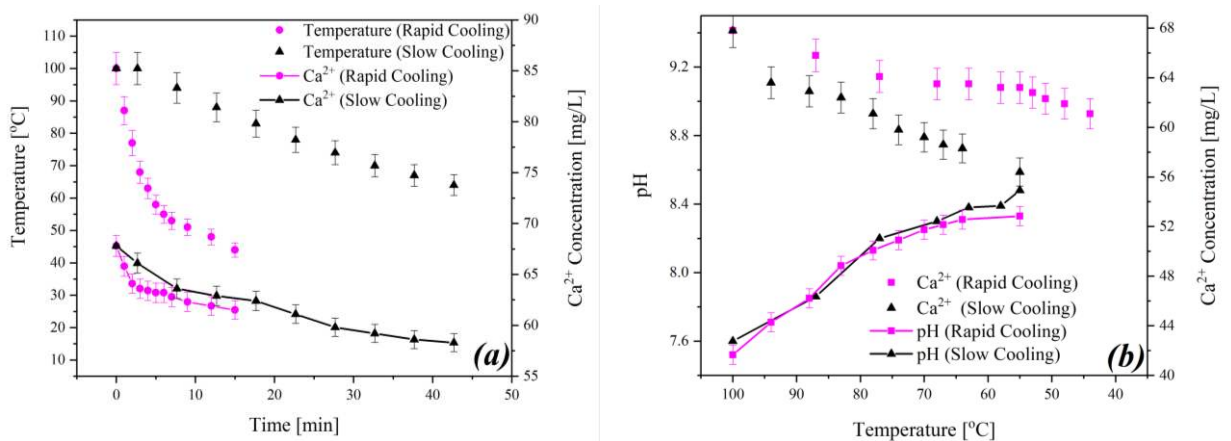


Fig. 6. (a) Change of temperature and calcium concentration with time, (b) change of pH and concentration with the temperature at different cooling rates.

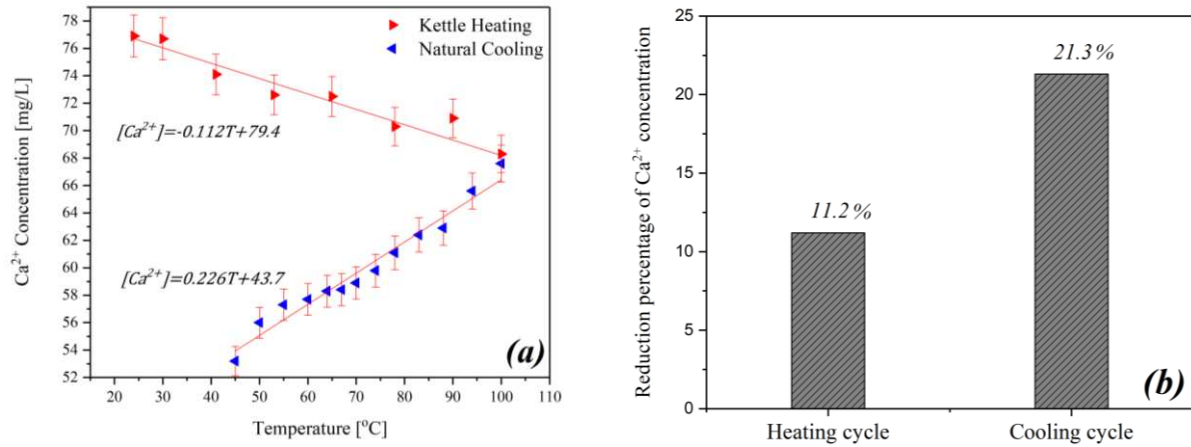


Fig. 7. (a) Change of calcium content with temperature, (b) the reduction percentage of calcium during the heating and cooling cycles.

The mass of calcium carbonate scale during heating and cooling cycles was theoretically estimated based on the precipitation rate model (Eq. 5) proposed by Morse [25]. Two assumptions were made in the calculations; concentrations of calcium and carbonate are kept constant during the process, and the precipitated crystals are calcite. The temperature profile used in the calculations is adopted from the heating and cooling experiments. The aim of these calculations is to estimate the scale amount if the scaling process is solely crystallisation reaction-controlled. In other words, the increase in the solution temperature enhances the solution saturation and hence the thermodynamic driving force of the scaling. Fig. 8a shows that the scale mass formed in the cooling cycle is greater than that in the heating cycle which supports the present findings. Both the time and supersaturation of solution in the cooling stage are higher than those in the heating stage. The ratios of $CaCO_3$ precipitated in the cooling cycle to the heating cycle from the experiments and theoretical calculations were compared. It can be seen in Fig. 8b that the theoretical ratio is greater than the experimental ratio because in the experiments the concentration of fouling species are consuming as a function of time. The consumption rate of calcium in the experimental cooling cycle is higher than that in the cooling cycle, as shown in Fig. 7a.

$$G = K (S - 1)^n \quad (5)$$

Where G is the precipitation rate, S is the saturation ratio, K is a rate constant and n is the order of reaction ($n=2$), as proposed by Opdyke *et al.* [26].

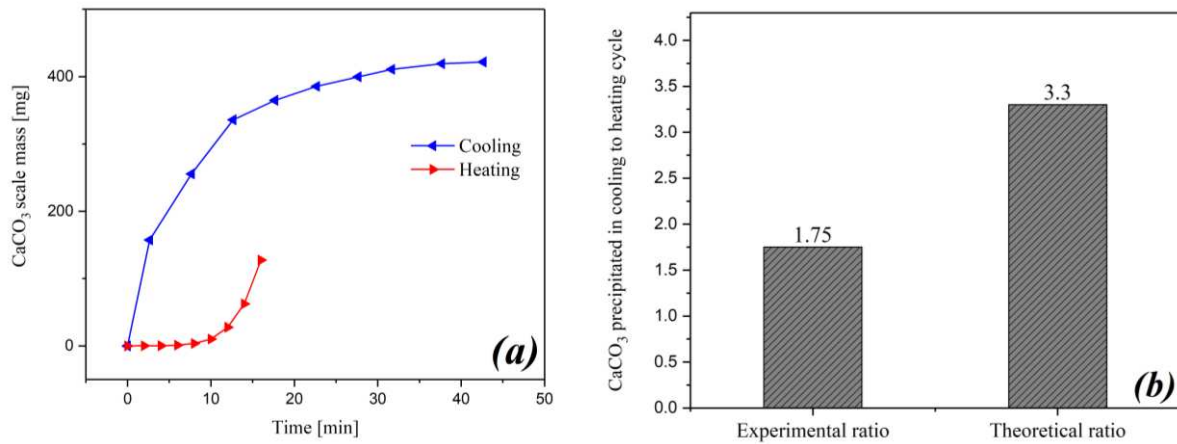


Fig. 8. (a) The theoretical profile of scale formation during the heating and cooling cycles, (b) experimental and theoretical cooling to heating scale ratios.

3.3. Effect of water composition

The formation of composite scale from tap water is predictable due to the presence of different fouling species. The change of calcium and sulphate ions has been examined as shown in Fig. 9. As such, there is no reduction in the concentration of Ca^{2+} and SO_4^{2-} occurring during the process of heating to 100 °C, no formation of CaSO_4 scale takes place. On the contrary, the content of the ions increases with time due to the water evaporation. As the solubility constant of calcium sulphate is higher than that of calcium carbonate, the reaction is not favourable at similar composition and temperature [27]. No precipitation has been noticed, despite the fact that the increase of temperature and concentrations of both ions which increases the saturation ratio from 0.3 to 7.9. This makes the formation of CaSO_4 from similar system and conditions unlikely to occur.

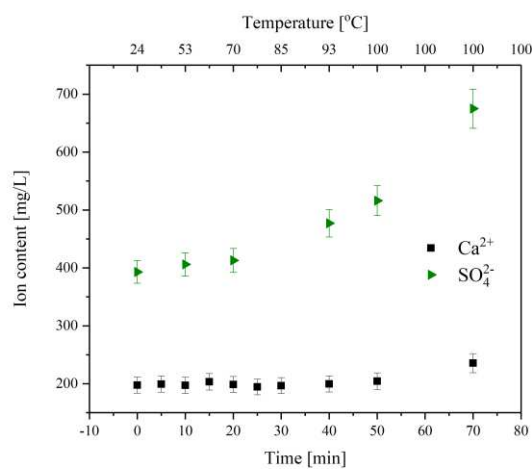


Fig. 9. Change of ion concentration in solution B during the heating process.

The presence of magnesium in water may contribute to the formation of different types of deposits such as magnesium oxide, magnesium hydroxide, and magnesium carbonate based on the operating conditions and composition [28, 29]. Fig. 10a shows how the content of magnesium changes in two different solutions. In solution C, no change in the magnesium content has been observed when the solution temperature is between about 25 and 60 °C. Then, as the temperature exceeded 60 °C, the content of magnesium starts to increase due to water evaporation. Upon reaching a critical saturation concentration, magnesium carbonate deposits form, the concentration of magnesium decreases due to the scaling reaction. For this water composition, the critical temperature for the magnesium scale to be formed is around 94 °C at a fixed heating rate. It can be seen that the consumption rate of Mg^{2+} in solution A is slower than solution C. The consumption rates of Mg^{2+} and Ca^{2+} in drinking water have been compared in Fig. 10b. The reduction in the concentration of Ca^{2+} is larger than Mg^{2+} , which illustrates that the calcium reaction rate is faster even at lower temperatures due to the low solubility of $CaCO_3$.

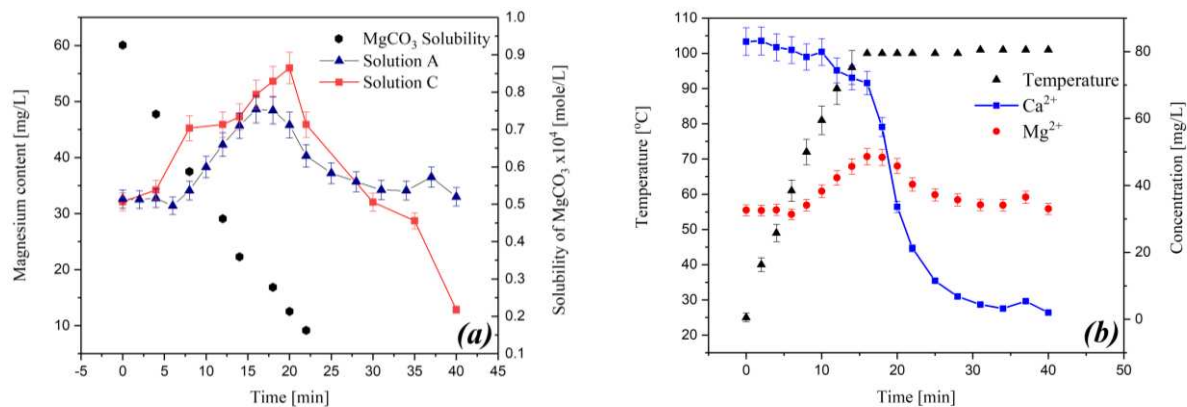


Fig. 10. (a) Change of $MgCO_3$ solubility with temperature, and magnesium content in different solutions, (b) the consumption rates of Mg^{2+} and Ca^{2+} in solution A, under the medium heating rate.

Fig. 11a displays the effect of magnesium content on the calcium precipitation rate with temperature. The lower the content of magnesium in the potable water the steeper the decrease of calcium at the same range of temperature and bicarbonate content. The concentration of calcium in the commercially bottled water (solution A) is not exactly identical. When it was measured by AAS, the initial concentration of calcium in solution A was ranging between 78 and 80.6 mg/L. The magnesium competes with calcium to form $MgCO_3$. This is confirmed by the ratio of magnesium to calcium concentrations, as displayed in Fig. 11b. The higher the initial concentration of magnesium the higher the consumption rate, and the less the carbonates to react with calcium.

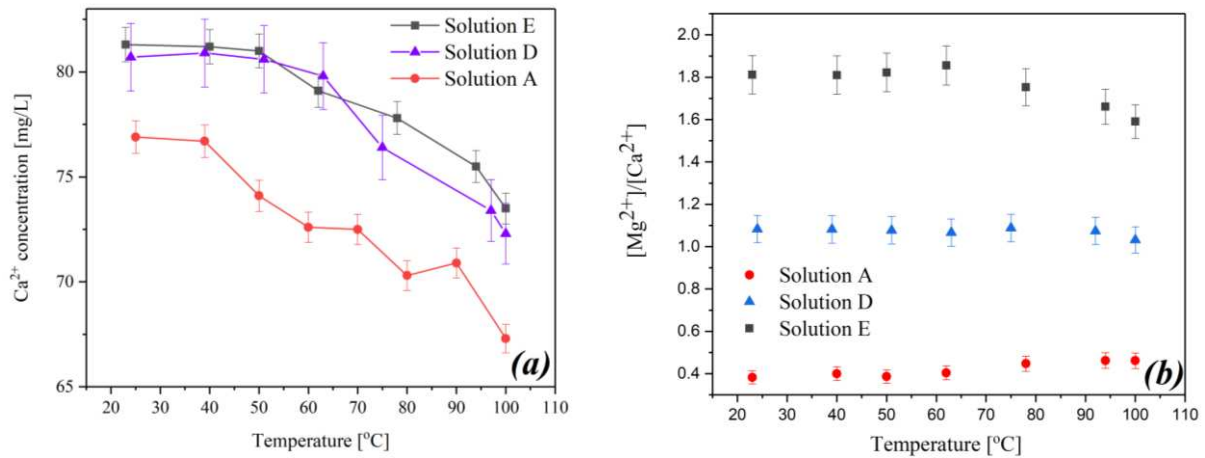


Fig. 11. (a) Calcium concentration change, (b) magnesium concentration change, with temperature at the different magnesium contents.

4. Conclusions

This paper has presented the precipitation kinetics of various types of inorganic scales during the heating and cooling processes relevant to the water in the domestic appliances. A series of experiments has been carried out to simulate the heating of tap water to boiling temperature followed by the normal cooling to ambient temperature. The effect of composition of water has also been studied.

The heating rate increases the rate of change of calcium reduction in a solution with time. However, the calcium concentration in solution when 100°C is attained at a rapid heating rate is higher than that at the same temperature at slow heating; a greater amount of scale formed when the solution is slowly heated. For the cooling stage, the faster the cooling rate the lower the rate of the calcium reduction in crystallisation reaction. Calcium carbonate formed in the cooling period was greater than in the heating period.

To check the probability of formation of calcium sulphate deposits under identical conditions, a solution of calcium and sulphate has been tested. The results showed that the solution content of calcium and sulphate increases with time and temperature as a consequence of water evaporation. As no reduction in the content of both species occurs even after 25 minutes at the boiling temperature, the formation of CaSO_4 is concluded to be unfavourable.

The concentration profile of magnesium, under the medium heating regime, is different when compared to the calcium profile. No change in the magnesium content has been observed when the solution temperature is between 25 and 60°C . Then, as the temperature exceeded 60°C , the content of magnesium starts to increase due to water evaporation. Finally, it decreases as soon as saturation concentration is achieved and it is thermodynamically sufficient for magnesium precipitate to form. The depletion rate of calcium is found to be affected by the content of magnesium for the same amount

of carbonate. The concentration of calcium steeply decreases with initial magnesium concentration decrease.

Acknowledgement

The authors acknowledge the funding and support from the Leeds University SALSAS consortium. We also acknowledge the financial support of the Leverhulme Trust Research Grant ECF-2016-204. We also wish to acknowledge the technical and administrative team of the Institute of Functional Surfaces (IFS), School of Mechanical Engineering at the University of Leeds for their supports.

References

- [1] Neville, A., *Surface Scaling in the Oil and Gas Sector: Understanding the Process and Means of Management*. Energy & Fuels, 2012. **26**(7): p. 4158-4166.
- [2] Setta, F.-A., and A. Neville, *Efficiency assessment of inhibitors on CaCO₃ precipitation kinetics in the bulk and deposition on a stainless steel surface (316 L)*. Desalination, 2011. **281**: p. 340-347.
- [3] Söhnel, O., and J. Mullin, *Precipitation of calcium carbonate*. Journal of Crystal Growth, 1982. **60**(2): p. 239-250.
- [4] Song, K.S., J. Lim, S. Yun, D. Kim, and Y. Kim, *Composite fouling characteristics of CaCO₃ and CaSO₄ in plate heat exchangers at various operating and geometric conditions*. International Journal of Heat and Mass Transfer, 2019. **136**: p. 555-562.
- [5] Sanni, O.S., O. Bukuaghangin, T.V. Charpentier, and A. Neville, *Evaluation of laboratory techniques for assessing scale inhibition efficiency*. Journal of Petroleum Science and Engineering, 2019: p. 106347.
- [6] Al-Gailani, A., T. Charpentier, O. Sanni, and A. Neville, *CRYSTALLIZATION FOULING IN DOMESTIC APPLIANCES AND SYSTEMS*. Heat Exchanger Fouling and Cleaning XIII - 2019.
- [7] Richards, C.S., F. Wang, W.C. Becker, and M.A. Edwards, *A 21st-Century Perspective on Calcium Carbonate Formation in Potable Water Systems*. Environmental Engineering Science, 2018. **35**(3): p. 143-158.
- [8] Whelton, A.J., A.M. Dietrich, G.A. Burlingame, M. Schechs, and S.E. Duncan, *Minerals in drinking water: impacts on taste and importance to consumer health*. Water Science and Technology, 2007. **55**(5): p. 283-291.

- [9] Khadsan, R., and M.V. Kadu, *Drinking Water Quality Analysis of Some Bore-Wells Water of Chikhli Town, Maharashtra*. I Control Pollution, 1970. **20**(1).
- [10] Chen, H., C. Qing, J. Zheng, Y. Liu, and G. Wu, *Synthesis of calcium carbonate using extract components of croaker gill as morphology and polymorph adjust control agent*. Materials Science and Engineering: C, 2016. **63**: p. 485-488.
- [11] Mwaba, M., C. Rindt, A. Van Steenhoven, and M. Vorstman, *Experimental investigation of CaSO₄ crystallization on a flat plate*. Heat transfer engineering, 2006. **27**(3): p. 42-54.
- [12] Raharjo, S., S. Muryanto, J. Jamari, and A.P. Bayuseno, *Controlling of magnesium carbonate scale deposition on the piping system with laminar flow and in the presence of alumina*. AIP Conference Proceedings, 2018. **1977**(1): p. 020064.
- [13] Gubbins, K.E., *Thermodynamics*. By K. S. Pitzer, 3rd ed., McGraw-Hill, New York, 1995, xvi+626 pp. AICHE Journal, 1997. **43**(1): p. 285-285.
- [14] Plummer, L.N., and E. Busenberg, *The solubilities of calcite, aragonite and vaterite in CO₂-H₂O solutions between 0 and 90 C, and an evaluation of the aqueous model for the system CaCO₃-CO₂-H₂O*. Geochimica et cosmochimica acta, 1982. **46**(6): p. 1011-1040.
- [15] Bénézeth, P., G.D. Saldi, J.-L. Dandurand, and J. Schott, *Experimental determination of the solubility product of magnesite at 50 to 200 C*. Chemical Geology, 2011. **286**(1-2): p. 21-31.
- [16] Arvidson, R.S., and F.T. Mackenzie, *Temperature dependence of mineral precipitation rates along the CaCO₃-MgCO₃ join*. Aquatic Geochemistry, 2000. **6**(2): p. 249-256.
- [17] Zhang, D., Q. Lin, N. Xue, P. Zhu, Z. Wang, W. Wang, Q. Ji, L. Dong, K. Yan, J. Wu, and X. Pan, *The kinetics, thermodynamics and mineral crystallography of CaCO₃ precipitation by dissolved organic matter and salinity*. Science of The Total Environment, 2019. **673**: p. 546-552.
- [18] Söhnel, O., and J. Garside, *Precipitation: basic principles and industrial applications*. 1992: Butterworth-Heinemann.
- [19] Chen, T., A. Neville, and M. Yuan, *Calcium carbonate scale formation—assessing the initial stages of precipitation and deposition*. Journal of Petroleum Science and Engineering, 2005. **46**(3): p. 185-194.
- [20] Al-Rawajfeh, A.E., H. Glade, and J. Ulrich, *Scaling in multiple-effect distillers: the role of CO₂ release*. Desalination, 2005. **182**(1-3): p. 209-219.
- [21] Prieto, F.J.M., and F.J. Millero, *The values of pK₁+ pK₂ for the dissociation of carbonic acid in seawater*. Geochimica et Cosmochimica Acta, 2002. **66**(14): p. 2529-2540.
- [22] Millero, F.J., and R.N. Roy, *A chemical equilibrium model for the carbonate system in natural waters*. Croatica chemica acta, 1997. **70**(1): p. 1-38.
- [23] Bott, T.R., *Fouling of heat exchangers*. 1995: Elsevier.

- [24] Andritsos, N., and A. Karabelas, *Calcium carbonate scaling in a plate heat exchanger in the presence of particles*. International Journal of Heat and Mass Transfer, 2003. **46**(24): p. 4613-4627.
- [25] Morse, J.W., *The kinetics of calcium carbonate dissolution and precipitation*. Reviews in Mineralogy and Geochemistry, 1983. **11**(1): p. 227-264.
- [26] Opdyke, B.N., and B.H. Wilkinson, *Carbonate mineral saturation state and cratonic limestone accumulation*. American Journal of Science, 1993. **293**(3): p. 217-234.
- [27] Marshall, W., and R. Slusher, *Solubility of Calcium Sulfate and its Hydrates in Sea Water and Saline Water Concentrates, and Temperature Concentration Limits*. Jour. Chem. & Eng. Data, 1968. **13**.
- [28] Raharjo, S., S. Muryanto, J. Jamari, and A. Bayuseno. *Controlling of magnesium carbonate scale deposition on the piping system with laminar flow and in the presence of alumina*. in *AIP Conference Proceedings*. 2018. AIP Publishing.
- [29] Dabir, B., R.W. Peters, and J.D. Stevens, *Precipitation kinetics of magnesium hydroxide in a scaling system*. Industrial & Engineering Chemistry Fundamentals, 1982. **21**(3): p. 298-305.